

# Thermal Stability and Mechanical Behavior of Cycloaliphatic–DGEBA Epoxy Blend System Initiated by Cationic Latent Catalyst

GEUN-HO KWAK, SOO-JIN PARK, JAE-ROCK LEE

Advanced Materials Division, Korea Research Institute of Chemical Technology, P.O. Box 107, Yusong, Taejeon 305-600, South Korea

Received 21 September 1999; accepted 3 December 1999

**ABSTRACT:** The effect of the composition of an epoxy blend based on a cycloaliphatic (CAE) and diglycidyl ether of bisphenol A (DGEBA) epoxides containing *N*-benzylpyrazinium hexafluoroantimonate (BPH) as a thermal or UV latent initiator was investigated in the context of their thermal stability and mechanical properties. The compositions of a CAE–DGEBA blend were varied within 100:0, 80:20, 60:40, 20:80, and 0:100 by mole percent. Latent properties were measured by the degree of conversion. As a result, the thermal stability characterized from the initial decomposition temperature (IDT), the temperature of maximum weight loss ( $T_{\max}$ ), the integral procedural decomposition temperature (IPDT), and the decomposition activation energies by TGA increased when the DGEBA composition was increased. According to the mechanical measurements, the flexural and tensile strengths increased with an increase of the DGEBA composition because of the compact hydrogen bond, long repeat unit, and bulky side groups of the DGEBA, while both the elastic and tensile moduli decreased. This latter result was attributed to the DGEBA intermolecular interaction, resulting in a toughened three-dimensional network, which dispersed the internal stress. © 2000 John Wiley & Sons, Inc. *J Appl Polym Sci* 78: 290–297, 2000

**Key words:** *N*-benzylpyrazinium hexafluoroantimonate (BPH); latent initiator; thermal stability; NIR; mechanical properties

## INTRODUCTION

Thermosetting materials have become increasingly important because of the wide variety of their applications in the automotive, electronics, aerospace, and plastic industries and in the making of structural composites.

Epoxy resins are prominent examples of such materials. Depending on the chemical structure of the curing agent and on conditions, it is possible to vary desired physical properties, such as toughness, chemical resistance, and mechanical

properties ranging from extreme flexibility to high strength, high adhesivity, good heat resistance, and high electrical resistance.<sup>1,2</sup> A curing agent or accelerator is necessary to promote the ring-opening polymerization of one or more of the terminal epoxide rings. Amines and diacid anhydrides are common curing agents. However, amine and anhydride agents are toxic and have low heat resistance and require high-energy consumption resulting from the long curing process at a high temperature.<sup>3</sup>

Recent years have seen an intensive study of cationic homopolymerization of plural epoxy resins.<sup>4,5</sup> In the cationic mechanism the epoxy group is opened by active hydrogen that is replaceable by a metal to produce a new physicochemical bond

Correspondence to: S.-J. Park (psjin@pado.kriect.re.kr).

*Journal of Applied Polymer Science*, Vol. 78, 290–297 (2000)  
© 2000 John Wiley & Sons, Inc.

or a hydroxyl group. The cationic initiator is generally used as a complex, such as  $\text{BF}_3$ -ether,  $\text{BF}_3$ -amine, or  $\text{SbF}_6$ -epoxide. This complex overcomes the disadvantages of excessively rapid gelation, high hygroscopicity, and light instability.<sup>6</sup> Particularly, development of latent catalyst for cationic polymerization is desirable for the enhancement of both the pot life and handling of thermosetting resins.<sup>7,8</sup> Usually, the latent catalyst forms an active species by external stimulation such as heat and photo-irradiation.

In practice, epoxy resins are often blended with other epoxy resins and with additives.<sup>9</sup> This is done to obtain better overall performance, such as ease of processing and good curing ability, high thermal stability, and strong mechanical strength, as well as good weatherability.

Near-infrared spectroscopy (NIR) provides a sample analysis with minimal technical effort and is a simple and reliable routine implementation. This arises from the small absorptivity of the overtone stretching and combination bands of the CH, NH, and OH groups.<sup>10</sup> It has been determined that the intensities of the epoxy and hydroxyl absorption bands follow the mechanisms of the reaction and the conversion.<sup>11</sup>

This article reports on the investigation of the effects of blend compositions composed of CAE and DGEBA initiated by a cationic latent type catalyst (i.e., *N*-benzylpyrazinium hexafluoroantimonate) on latency, thermostability, and mechanical behavior.

## EXPERIMENTAL

### Materials and Sample Preparation

The two types of epoxy resins used in this work were diglycidyl ether of bisphenol A (DGEBA, LY556 supplied by the Ciba-Geigy Co.) and cycloaliphatic epoxy (CAE, ERL4221 supplied by the Union Carbide Co.). Cationic latent catalyst (BPH) for the present investigation was synthesized through the reaction from pyrazine, benzyl bromide, and  $\text{NaSbF}_6$ .<sup>12</sup> Figure 1 shows the structural formulas of both monomers and BPH. The chemical analyses of BPH are shown in Table I.

The BPH was dissolved in DGEBA, and then CAE was added to the DGEBA-BPH mixture, in 20% increments between 0 and 100 mol %. All formulations were mixed at room temperature and degassed under a vacuum for 1 h to remove voids and residual organic solvents. The bubble-

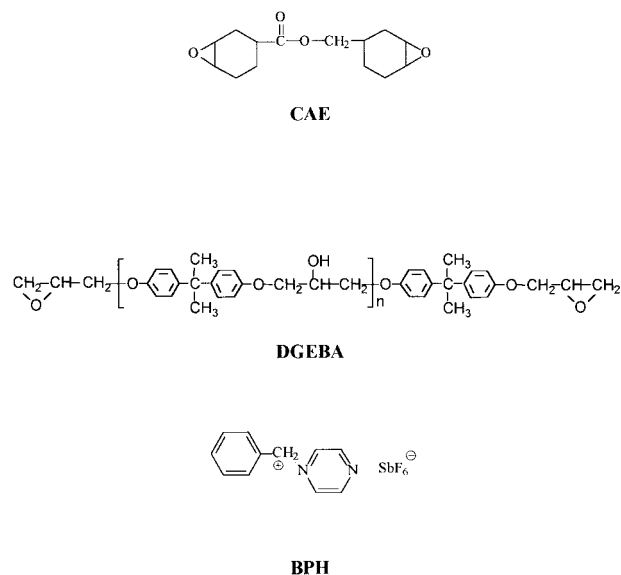


**Figure 1** Chemical structures of CAE, DGEBA and BPH.

free mixture was poured into a stainless-steel mold and cured at 70°C for 30 min, then 140°C for 2 h, and it was finally postcured at 200°C for 1 h.

### Latent Properties

Evaluations of latent properties were performed by the measurement of conversion as a function of reaction time, using a Du Pont DSC910 supported by a Du Pont thermal analyzer at 50°C and 150°C. A mixture of the epoxy and BPH was poured into an UV-transparent glass mold and was then irradiated with a 400 W high-pressure halide lamp, always maintaining the same distance between the lamp and the specimen, equal to 10 cm, to obtain measurement of UV latent properties. The degree of conversion of the UV-cured system was evaluated by the peak at  $915\text{cm}^{-1}$  of FTIR.<sup>13</sup>

### Thermal Stability and Mechanical Behavior

The thermogravimetric analyses were performed in nitrogen using a TGA 951 Du Pont thermal analyzer, at a heating rate of 10°C/min from 35 to 800°C to investigate the thermal stability of the cured resins.

An Instron tester (Model 1125) was used to measure flexural properties of the CAE-DGEBA-BPH system according to ASTM D-790. The flexural specimens were cut in pieces 80 mm long, 12.7 mm wide, and 3 mm thick. The span-to-depth ratio was 16:1, and crosshead speed was 2 mm/min.

**Table I** Chemical Analyses of BPH

Analysis Method	Analysis	
FT-IR (KBr)	peaks ( $\text{cm}^{-1}$ )	1514, 1358, 1223, 1073, 1015, 767, 726, 662
$^1\text{H}$ NMR	Pyridine aromatic ring $-\text{CH}_2-$	9.33–9.38, 9.65–9.70 7.70–7.47 6.18
Elemental analysis	Calculated for $\text{C}_{11}\text{H}_{11}\text{N}_2\text{SbF}_6$ found	C: 32.45%, H: 2.70%, N: 6.88% C: 32.90%, H: 2.74%, N: 6.91%

Tensile properties were measured on an Instron Universal Testing Machine (Model 1125) according to ASTM D638 at a crosshead speed of 1 mm/min and a strain-gauge length of 50 mm. A strain gauge extensometer was applied to measure longitudinal strains. The load and displacement were recorded simultaneously. The tensile modulus was taken from the initial linear region of the stress-strain curve.

## RESULTS AND DISCUSSION

### Latent Properties

Figure 2 shows conversion as a function of the curing time for the different compositions of the blends made with 1 mol % BPH initiator by isothermal DSC. As the curing proceeds, the degree of conversion increases with increasing DGEBA content in the case of the 150°C reaction temperature. On the other hand, the conversion in the 50°C reaction temperature shows no significant

evolution after 2 h. This is because of the low temperature, which has become a limiting factor prohibiting the activity of catalyst. It means that BPH has a thermostable latent peculiarity at a given temperature condition in spite of the presence of external heat stimulation.

Figures 3 and 4 show the infrared spectra of UV-cured CAE-BPH and DGEBA-BPH respectively during curing at room temperature. The hydroxyl absorption band and epoxide band occurred at  $3500\text{cm}^{-1}$  and  $915\text{cm}^{-1}$ , respectively. For the hydroxyl peak of the CAE-BPH system, as seen in Figure 3, the peak intensity was nearly constant during the curing, while the epoxide peak intensity sharply decreased with increasing cure time. But, as seen in Figure 4, the intensity of the hydroxyl band increased with increased cure time, which means more possibility of crosslinking than that of Figure 3. In the case of Figure 4, the curing process may lead to a compact network structure, inducing changes in activated hydroxyl groups to intermolecular hydrogen

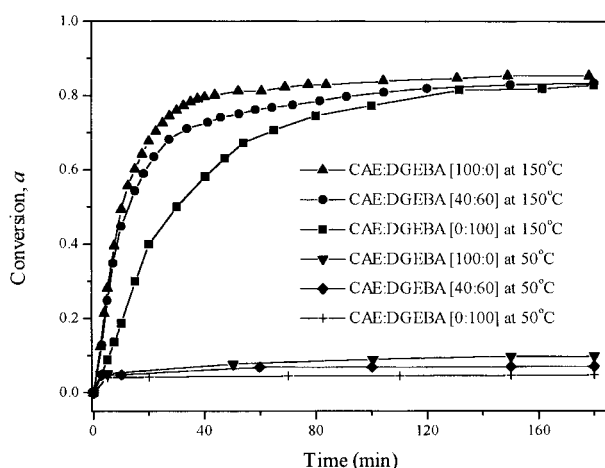


**Figure 2** Time-conversion curves of the CAE-DGEBA-BPH system at 150°C and 50°C with curing time.

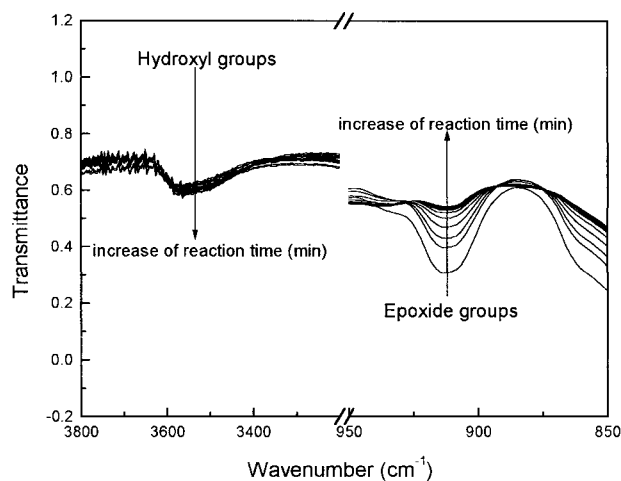


**Figure 3** FTIR spectra of the CAE-BPH system as a function of reaction time.

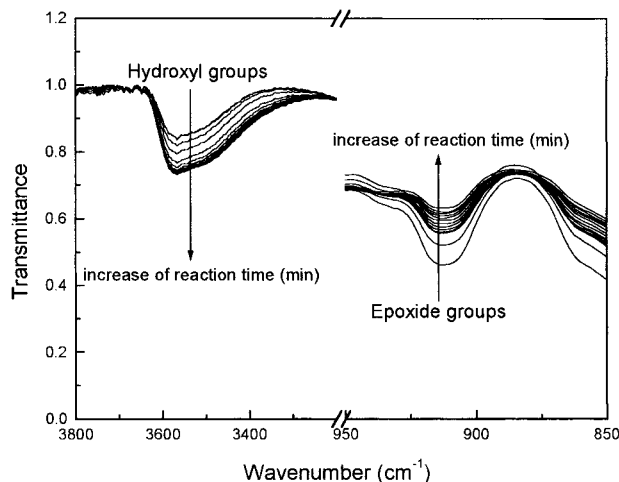


**Figure 4** FTIR spectra of the DGEBA-BPH system as a function of reaction time.

bonding.<sup>13</sup> In addition, the epoxide band of the DGEBA-BPH system sharply decreases with reaction time as compared with that of the CAE-BPH.

The hydroxyl groups resulted from the cleavage of the oxirane rings by the catalyst or activated sites. In addition to the hydroxyl groups attached to the backbone of the epoxy oligomer, more hydroxyl groups were produced by ring opening during cure. Thus, a number of hydroxyl groups underwent nucleophilic addition reactions with epoxide, resulting in ring cleavage and the formation of increased crosslinking network

It is well known that conversion behaviors for curing epoxy resins with catalyst are complex because of the involvement of epoxy-catalyst, hydroxyl-epoxy, and side reactions.<sup>14</sup> These reactions, which occur during the crosslinking of the resin, change the properties of the epoxy network.<sup>15</sup> Interpretation of NIR spectra by correlation with chemical species is very complex and difficult. However, FTIR measurement of polymeric materials provides a highly precise analysis of cure kinetics that is widely interpretable in terms of chemical structure.<sup>16</sup> In a conversion study, the degree of conversion of epoxy resin can be evaluated by the disappearance of the peak at  $915\text{cm}^{-1}$ ,<sup>15-20</sup> and it can be expressed as:

$$\alpha_{E(t)} = 1 - \frac{(A_{915}/A_{1510})_{t=t}}{(A_{915}/A_{1510})_{t=0}} \quad (1)$$

where,  $A_{915}$  and  $A_{1510}$  are the peak areas, respectively, for epoxide and aromatic C—H as reference bands in this system.

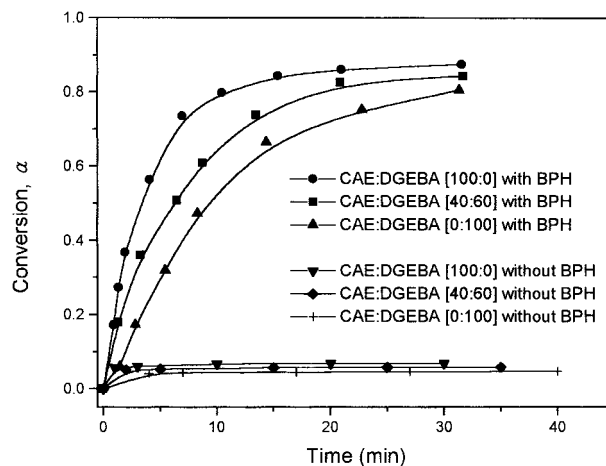
The relationship between the conversion of epoxide groups and cure time obtained from the peak area for epoxide is shown in Figure 5. As a result, the conversion rate and reactivity increased by increasing the CAE composition with BPH catalyst. Therefore, it is clear that BPH acts as a UV latent initiator, and the reactivity in the degree of the CAE conversion is superior to that in the degree of the DGEBA conversion.

Figure 6 shows selected NIR spectra of a hydroxyl group as increasing reaction times of the CAE-DGEBA blend system at different compositions varied within 100:0, 40:60, and 0:100 mol % at  $100^\circ\text{C}$ . The first overtone of the hydroxyl group stretching as a result of reaction temperature and time increases was found at  $7100\text{cm}^{-1}$ . The use of this band to monitor reaction kinetics in terms of the appearance of a hydroxyl group has been a successful way to quantify epoxy cure reactions.<sup>18</sup>

The use of NIR diffuse reflectance spectroscopy for quantitative analysis is now widely accepted. Various mathematical models of calibration standards have been developed to correlate concentration to spectroscopic data, usually to express the common logarithm of the inversion of reflectance ( $\log 1/R_f$ ) for each wavelength studied. If the sample absorbs at the same wavelengths, ( $\log 1/R_f$ ) appears to be the best method to relate reflectance to concentration, as follows:<sup>18</sup>

$$R_f = \frac{I_s}{I_r} \quad (2)$$

where  $R_f$  is the reflectance;  $I_s$ , the intensity of sample; and  $I_r$ , the internal reference.



**Figure 5** Time-conversion curves of the CAE-DGEBA system at room temperature with and without BPH, as a function of curing time obtained from FTIR.

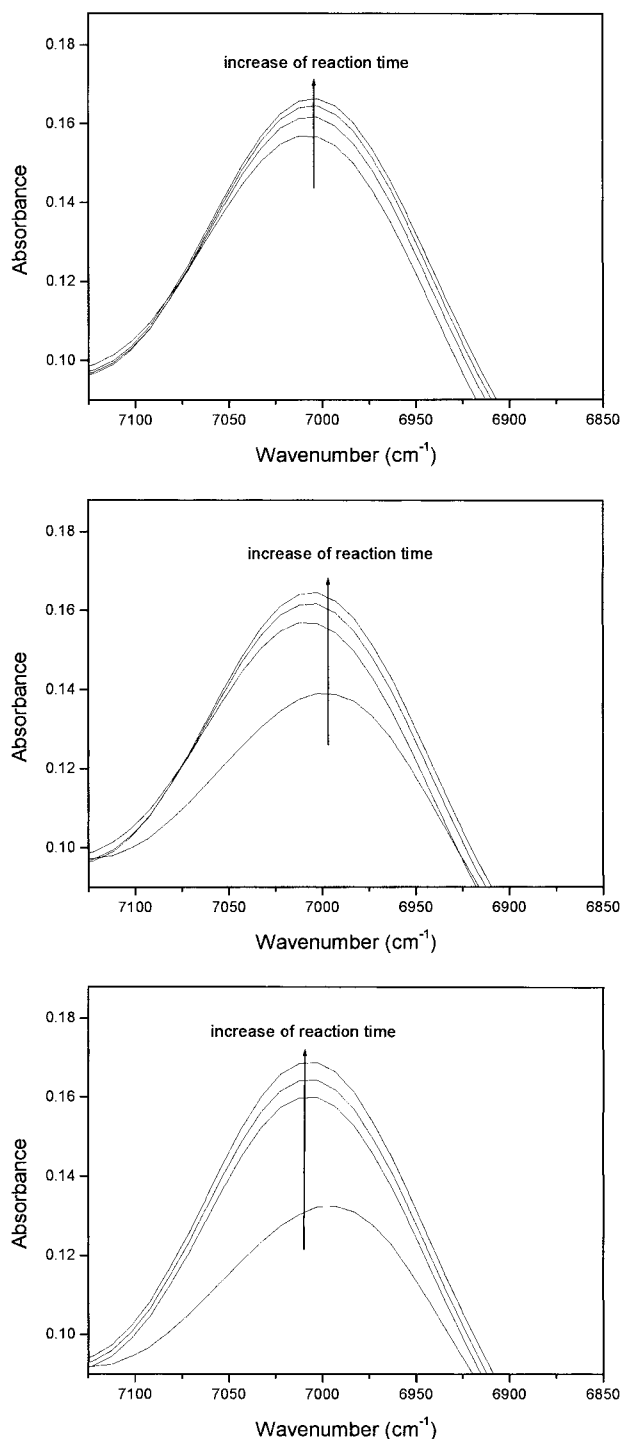


**Figure 6** Changes in hydroxyl absorbencies with reaction time of the CAE-DGEBA-BPH system measured at 100°C with different compositions: (a) 100:0, (b) 40:60, and (c) 0:100.

Figure 7 represents the conversion of hydroxyl groups calculated from eq. (2) with different blend compositions monitored by changes in the inten-

sity of each time-dependent band. When the kinetic results of this system were compared, the kinetics of the reaction groups in the NIR spectra were found to differ in conversions and in reproducible trends. The three curves of extent of reaction for a given temperature appear horizontally shifted with respect to one another but maintain similar slopes. The autocatalytic nature of all the curves is apparent. As the experimental results show, the conversion of hydroxyl groups increases with increasing content of DGEBA and shows a similar tendency in the case of FTIR analysis.

### Thermal Stabilities

It is well known that one of the basic requirements in the multicomponent epoxy system is to have a homogeneous mixture prior to the curing process.<sup>6,16</sup> Thermograms of epoxy resins prepared from blending different compositions of CAE are superimposed on Figure 8. Decomposition curve behaviors are largely similar to whatever CAE composition may be considered, which means an uncured homogeneous mixture without apparent phase separation is prepared in this system.

The results of the experiment showed some factors of thermal stability, including initial decomposition temperature (IDT), temperature of maximum rate of weight loss ( $T_{max}$ ), and integral procedural decomposition temperature (IPDT),<sup>21</sup> had increased values with an increasing concentration of DGEBA in blends, as shown in Table II.

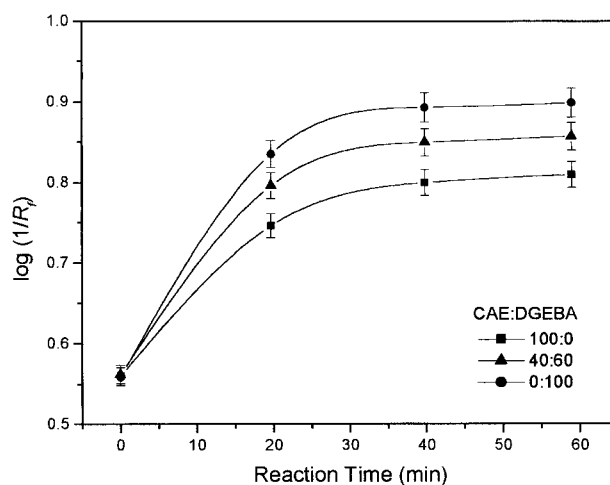


**Figure 7** Conversion of hydroxyl absorbencies with reaction time of the CAE-DGEBA-BPH system measured at 100°C with different compositions.



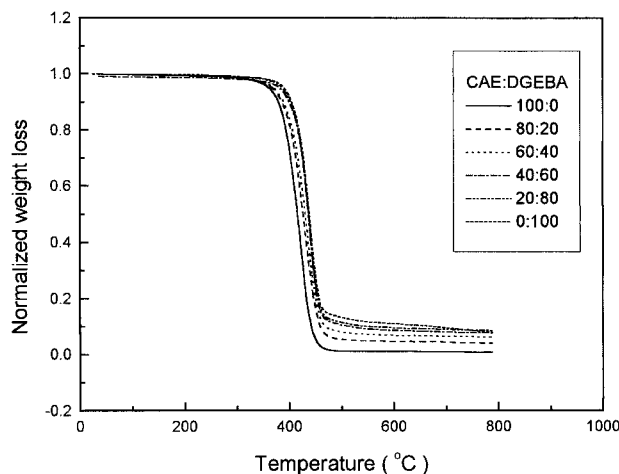


**Figure 8** TGA thermograms of the CAE-DGEBA-BPH system.

This can be explained by the inherent chemical structures, such as a bulk side group including a long unit, a stable aromatic ring, and increasing the interaction between the hydroxyl-functional group of DGEBA and BPH.

It is noted that thermal degradation progresses by etherification and subsequently proceeds via dehydration and thermal oxidation, which results in the scission of network chains.<sup>22,23</sup> Through this behavior it is possible to measure the energy of activation for the decomposition of resins. Decomposition activation energy,  $E_a$ , is calculated from TGA curves using the integral method of Horowitz and Metzger,<sup>4</sup> as follows:

$$\ln[\ln(1 - \alpha)^{-1}] = \frac{E_a \theta}{RT_{\max}^2} \quad (3)$$

where  $\alpha$  is the decomposition fraction,  $T_{\max}$  is temperature of maximum rate of weight loss,  $\phi$  is  $T - T_{\max}$ , and  $R$  is the gas constant.

**Table II** Thermal Stabilities of CAE-DGEBA-BPH Blend System by TGA

Compositions [CAE : DGEBA]	IDT [°C]	$T_{\max}$ [°C]	IPDT [°C]
[100 : 0]	290	420	428
[80 : 20]	299	428	457
[60 : 40]	312	434	488
[40 : 60]	317	446	512
[20 : 80]	336	448	552
[0 : 100]	353	450	589

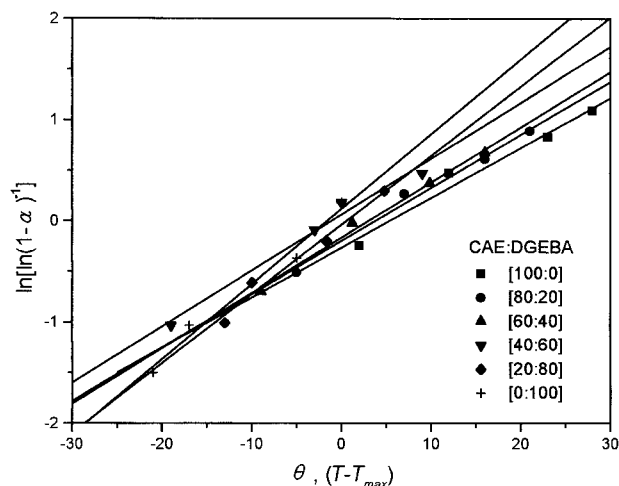


**Figure 9** Plot of  $\ln[\ln(1 - \alpha)^{-1}]$  versus  $\phi$  for CAE-DGEBA-BPH system.

The plots of  $\ln[\ln(1 - \alpha)^{-1}]$  versus  $\phi$  are shown in Figure 9. From the slope of these straight lines, the decomposition activation energy of the blend was determined in eq. (3). As shown in Table III, it was observed that the decomposition activation energy increases by increasing the DGEBA composition, which could be influenced by the volume fraction of a hard segment, such as an aromatic rings and imide groups, hydrogen bonds, repeat units, and thermal history.<sup>25,26</sup> Therefore, the observations of Table III result from the chemical nature of DGEBA and show good reliability compared with previous cure kinetics and quantitative analysis using FTIR and NIR, respectively.

### Mechanical Properties

The mechanical properties of this epoxy blend system were determined in terms of flexural strength,  $\sigma_f$ ; elastic modulus,  $E_b$ ; flexure, tensile strength,  $\sigma_t$ ; and tensile modulus,  $E_t$ . The  $\sigma_f$  and  $E_b$  for the cured specimens determined from three-point bending tests were calculated using the following equations:

$$\sigma_f = \frac{3PL}{2bd^2} \quad (4)$$

$$E_b = \frac{L^3 P}{4bd^3 m} \quad (5)$$

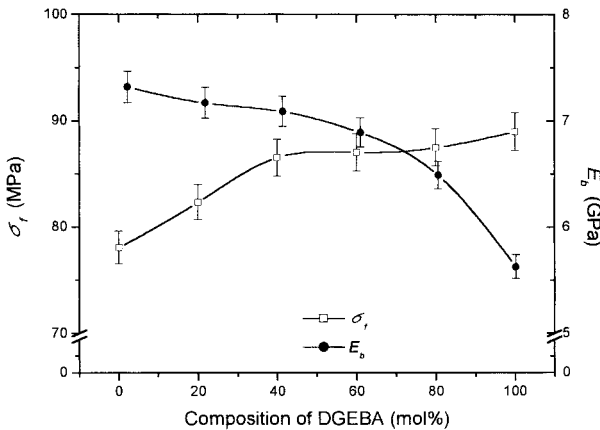
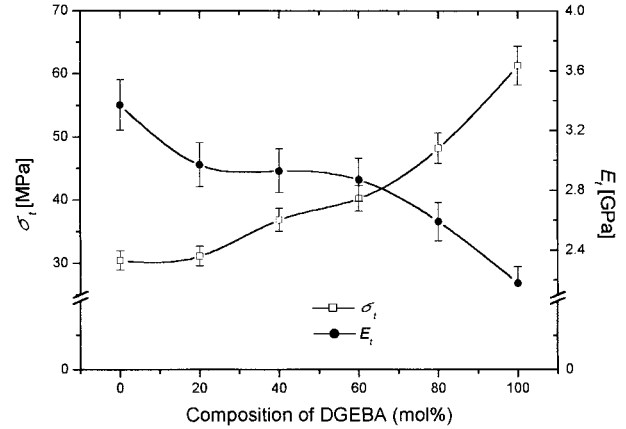
where  $P$  is load (N),  $L$  is span length (m),  $b$  is width of specimen (m),  $d$  is thickness of specimen (m),  $\Delta P$  is change in force in the linear portion of

**Table III** Decomposition Activation Energies of CAE-DGEBA Blend System

Compositions [CAE : DGEBA] [mol %]	$\ln[\ln(1 - \alpha)^{-1}]$	$\theta$	$E_a$ [kJ/mol]
[100 : 0]	-0.2450	2	197
	0.4760	12	
	0.8340	23	
	1.0972	28	
[80 : 20]	-0.5058	-5	218
	0.2716	7	
	0.6139	16	
	0.8923	21	
[60 : 40]	-0.7000	-9	228
	-0.0204	1	
	0.3759	9	
	0.6812	16	
[40 : 60]	-1.0309	-19	238
	-0.0874	-3	
	0.1856	0	
	0.4759	9	
[20 : 80]	-1.0035	-13	295
	-0.6073	-10	
	-0.1950	-1.6	
	0.3014	4.8	
[0 : 100]	-1.5000	-21	322
	-1.0309	-17	
	-0.3665	-5	
	0.1856	0	

the load-deflection curve (N), and  $\Delta m$  is change in deflection corresponding to  $\Delta P$  (m).

Figure 10 shows the flexural strength and the elastic modulus in flexure as a function of DGEBA

**Figure 10** Flexural strength and elastic modulus in flexure of the cured specimens as a function of the composition of DGEBA.**Figure 11** Tensile strength and modulus of the cured specimens as a function of the composition of DGEBA.

composition. As shown in the figure, the relative error is below 5%, which means the present data is very reliable. The flexural strength increased with increasing the DGEBA composition, the result of a compact hydrogen bond by the hydroxyl groups and a long repeat unit containing bulky side groups. On the other hand, the elastic modulus decreased as DGEBA increased. The decrease of elastic modulus resulted from the inherent nature of DGEBA because the hydroxyl groups of the DGEBA play an important role in enhancing the epoxide-activated site interaction and help in decreasing the elastic modulus, itself a result of to effective stress transfer.<sup>27,28</sup>

Tensile strength ( $\sigma_t$ ) and tensile modulus ( $E_t$ ) are calculated from following equations:

$$\sigma_t = \frac{P}{A} \quad (6)$$

$$E_t = \frac{P}{A} \cdot \frac{L_0}{\Delta L} \quad (7)$$

where  $A$  is the cross-sectional area for the specimen ( $m^2$ ) and  $L_0/\Delta L$  is the degree of sample elongation.

The tensile properties evaluated from the stress-strain curves are presented in Figure 11. It can be observed that tensile strength systematically increased as DGEBA composition increased, while tensile modulus of the cured resin drastically decreased. The measurements between flexural and tensile test exhibited different values but showed a similar tendency when the DGEBA content increased. The difference may be result from the mode of stress experienced by the

specimen. In the case of flexural testing, it is a combination of compression and tensile, while in tensile testing it is purely tensile.<sup>29</sup> It is known that factors influencing the strength and modulus properties are orientation, interfacial interaction, and the nature of chemical structure.<sup>28</sup> Therefore, the cure behavior and the chemical structure of the DGEBA can also explain these tensile properties. DGEBA shows an increase in hydroxyl groups during cure reaction, as shown in Figures 4 and 6, and is able to form a higher intermolecular interaction than that of the CAE. This makes it possible to produce a high network structure, resulting in improved tensile strength. The chain segments responsible for entanglements and intermolecular interactions, such as hydrogen bonding and double helical formations, are most likely the outer bulky side chains, which is related to free volume including the hydroxyl groups of DGEBA.<sup>27</sup> As a result, as the composition of DGEBA increases, the intermolecular bonding toughens the three-dimensional structure and consequently disperses the internal stress, which results in decreasing the tensile modulus.<sup>28-30</sup>

## CONCLUSION

In this work, the latency, thermostability, and mechanical properties of blends of CAE-DGEBA-BPH were studied using DSC, FTIR, NIR, TGA, and three-point bending and tensile mechanical tests.

The cationic catalyst acts as a thermal or a latent UV-activated initiator during the curing reaction. The reactivity and conversion rate increase with increasing CAE composition. As observed from thermal and mechanical properties, increasing the composition of DGEBA containing long repeat units, bulk side groups, stable aromatic ring structures, and reactive hydroxyl functional groups can form well-developed three-dimensional networks and can be correlated with the results of the thermal stabilities and mechanical strength properties. Increasing the composition of DGEBA plays an important role in decreasing both elastic and tensile modulus. This is a consequence of the toughened network structure and free volume, resulting from bulky side groups, which are able to disperse the internal stress.

## REFERENCES

1. Bauer, R. S. *Epoxy Resin Chemistry*; American Chemical Society: Washington, DC, 1979.
2. Lee, H.; Neville, K. *Handbook of Epoxy Resins*; McGraw: New York, 1967.
3. Inoue, S.; Aida, T. *Ring-Opening Polymerization*; Elsevier: New York, 1984; Vol. I.
4. Lee, S. D.; Takata, T.; Endo, T. *Macromolecules* 1996, 29, 3317.
5. Abu-Abdoun, I. I.; Ali, A. *Eur Polym J* 1992, 28, 73.
6. May, C. A. *Epoxy Resins*, 2nd ed.; Marcel Dekker: New York, 1988.
7. Crivello, J. V.; Lam, J. H. *J Polym Sci, Polym Chem* 1980, 18, 1021.
8. Gu, J.; Narang, S. C.; Pearce, E. M. *J Appl Polym Sci* 1985, 30, 2997.
9. Lin, S. T.; Huang, S. K. *J Polym Sci, Polym Chem* 1996, 34, 1907.
10. Poisson, N.; Lachenal, G.; Sautereau, H. *Vib Spec* 1996, 12, 237.
11. Mijovic, J.; Andjelic, S. *Macromolecules* 1995, 28, 2787.
12. Kim, Y. C.; Park, S. J.; Lee, J. R. *Polym J* 1997, 29, 759.
13. Lachenal, G.; Pierre, A.; Poisson, N. *Micron* 1996, 27, 1329.
14. Ochi, M.; Tsuyuno, N.; Sakaga, K.; Nakanishi, Y.; Murata, Y. *J Appl Polym Sci* 1995, 56, 1161.
15. Tokizawa, M.; Okada, H.; Wakabayashi, N. *J Appl Polym Sci* 1993, 50, 875.
16. Elias, H. G. *An Introduction to Polymer Science*; VCH Pub.: New York, 1997.
17. Wang, X.; Gillham, J. K. *J Appl Polym Sci* 1991, 43, 2267.
18. Xu, L.; Schlup, J. R. *J Adv. Mater* 1997, 28, 47.
19. Lin, Y. G.; Sautereau, H.; Pascault, J. P. *J Polym Sci, Polym Chem Eng* 1986, 24, 2171.
20. Skourlis, T. P.; McCullough, R. L. *J Appl Polym Sci* 1996, 62, 481.
21. Kwak, G. H.; Park, S. J.; Lee, J. R.; Hong, S. K. *Polymer (Korea)* 1999, 23, 281.
22. Hourston, D. J.; Lane, J. M. *Polymer* 1992, 33, 1379.
23. Lee, L. H. *J Polym Sci* 1965, 3, 895.
24. Horowitz, H. H.; Metzger, G. *Anal Chem* 1963, 35, 1464.
25. Samuels, S. L.; Wilkes, G. L. *J Polym Sci, Polym Symp* 1978, 43, 149.
26. Wilkes, G. L.; Moody, P. C.; Tant, M. R. *Polym Eng Sci* 1979, 19, 1029.
27. Van Soest, J. J. G.; De Wit, D.; Vliegthart, J. F. G. *J Appl Polym Sci* 1996, 61, 1927.
28. Bajaj, P.; Jha, N. K.; Kumar, R. A. *J Appl Polym Sci* 1992, 44, 1921.
29. Dowling, N. E. *Mechanical Behavior of Materials*; Prentice Hall: New Jersey, 1993.
30. Maiti, S. N.; Mahapatro, P. K. *J Appl Polym Sci* 1991, 42, 3101.